JLB

Article

Reduced transcript stabilization restricts TNF-α expression in RAW264.7 macrophages infected with pathogenic mycobacteria: evidence for an involvement of lipomannan

Tina Basler, Helmut Holtmann,† Jens Abel,* Torsten Eckstein,‡ Wolfgang Bäumer,§ Peter Valentin-Weigand,* and Ralph Goethe*,1*

Institut für *Mikrobiologie and Institut für §Pharmakologie, Stiftung Tierärztliche Hochschule Hannover, Hannover, Germany; †Institut für Biochemie, Medizinische Hochschule Hannover, Hannover, Germany; and ‡Department of Microbiology, Immunology, and Pathology, Colorado State University, Ft. Collins, Colorado, USA

RECEIVED MARCH 27, 2009; REVISED SEPTEMBER 10, 2009; ACCEPTED SEPTEMBER 11, 2009. DOI: 10.1189/jlb.0309207

ABSTRACT

Despite the critical role that TNF-α plays in the containment of mycobacterial infection, the mechanisms involved in regulation of its expression by mycobacteria are poorly defined. We addressed this question by studying MAP, which causes a chronic enteritis in ruminants and is linked to human Crohn's disease. We found that in MAP-infected macrophages, TNF-α gene expression was substantially lower than in macrophages infected with nonpathogenic MS or stimulated with LPS. TNF-α transcription alone could not fully explain the differential TNF-α mRNA expression, suggesting that there must be a substantial contribution by post-transcriptional mechanisms. Accordingly, we found reduced TNF-α mRNA stability in MAP-infected macrophages. Further comparison of MAP- and MS-infected macrophages revealed that lower TNF-α mRNA stability combined with lower mRNA and protein expression in MAP-infected macrophages correlated with lower p38 MAPK phosphorylation. Theses findings were independent of viability of MAP and MS. We demonstrate that the major mycobacterial cell-wall lipoglycan LM of MAP and MS induced TNF-α mRNA transcription, but only the MS-LM induced p38 MAPK-dependent transcript stabilization. Overall, our data suggest that pathogenic mycobacteria cause weak p38 MAPK activation and TNF-α mRNA stabilization as a result of their structural cell-wall components such as LM and thereby, restrict TNF-α expression in macrophages. *J. Leukoc. Biol.* 87: 173–183; 2010.

Introduction

Pathogenic mycobacterial species, such as *Mycobacterium avium* ssp., *Mycobacterium bovis, Mycobacterium leprae*, and MTB, persist in macrophages, causing granuloma formation or granulomatous inflammation in different host tissues. One of the key players of this host reaction is the proinflammatory cytokine TNF-α [1–3]. As a central factor of inflammatory responses, TNF-α also contributes to pathogenesis of other chronic inflammatory diseases such as rheumatoid arthritis and Crohn's disease [4–6].

In mycobacterial infection, TNF-α is involved in the regulation of apoptosis and dendritic cell maturation and together with IFN-γ, in the induction of antimicrobial activity of macrophages [6]. Furthermore, TNF-α plays an important role in the inhibition of mycobacterial growth in vitro [7, 8]. However, TNF-α responses of macrophages infected with pathogenic mycobacteria seemed to be reduced when compared with nonpathogenic or attenuated mycobacteria [9–13]. This might be a result of structural differences of mycobacterial cell-wall components. LAM and LM are integral parts of the mycobacterial cell wall recognized by cells involved in the innate immune response and have been found to modulate the cytokine response [14]. LAM and LM have been shown to induce TNF-α release in macrophages; however, LM is more potent [15, 16].

Despite the critical role that TNF-α plays in the containment of mycobacterial infection, the mechanisms involved in regulation of its expression by pathogenic mycobacteria are poorly defined. Biosynthesis of TNF-α is tightly controlled at the transcriptional [17–21] and post-transcriptional level [22–24]. The transcriptional initiation of the TNF-α gene serves as the pri-

Abbreviations: ARE=adenosine-uridine-rich element, LAM=lipoarabinomannan(s), LM=lipomannan(s), MAA=*Mycobacterium avium* subspecies *avium*, ManLAM=mannose-capped LAM, MAP=*Mycobacterium avium* subspecies *paratuberculosis*, MK2=MAPK-activated protein kinase 2, MOI=multiplicities of infection, MS=*Mycobacterium smegmatis*, MTB=*Mycobacterium tuberculosis*, $OD_{660\ nm}$=OD at 660 nm, PILAM=phosphoinositol-capped LAM, PT=primary transcript, qRT-PCR=quantitative RT-PCR, ssp.=subspecies

1. Correspondence: Institut für Mikrobiologie, Zentrum für Infektionsmedizin, Stiftung Tierärztliche Hochschule Hannover, Bischofsholer Damm 15, Germany. E-mail: ralph.goethe@tiho-hannover.de

mary control of the regulation of TNF-α production, and many transcription factors are known to be recruited to the TNF-α promoter [17–21]. However, it was reported that activation of macrophages with LPS results in an increase of transcription of only approximately threefold, and protein synthesis is increased ~10,000-fold [4]. Thus, the regulation of TNF-α expression in LPS-treated macrophages is regulated, to a large extent, post-transcriptionally [4].

The TNF-α 3′-untranslated region contains an ARE, which is involved in control of mRNA translation and stability as a result of the binding of specific *trans*-acting proteins [25]. The regulation and the coordinated interaction of these *trans*-acting proteins with the TNF-α ARE, leading to modulation of mRNA stability, are incompletely understood. The p38 MAPK and the downstream kinases MK2 are of major importance. TNF-α mRNA stabilization in LPS-stimulated macrophages is abolished when p38 MAPK is inhibited by its specific inhibitor SB203580 [26]. Nevertheless, the precise mechanisms of p38-dependent regulation of TNF-α mRNA stability remain to be fully elucidated.

Among pathogenic mycobacteria, the ruminant pathogen MAP is frequently hypothesized as the etiological agent of the chronic inflammatory bowel condition of humans called Crohn's disease [27]. In ruminants, MAP causes paratuberculosis (Johne's disease), a chronic granulomatous inflammation of the small intestine. The disease occurs worldwide, causing substantial economic losses in farms as a result of premature culling and production losses [28]. In paratuberculosis, TNF-α expression seems to be reduced specifically at the sites of MAP infection through unknown mechanisms [29]. Furthermore, the activity of TNF-α in cell culture supernatants of bovine macrophages was lower in MAP-infected cell cultures compared with IFN-γ and LPS-stimulated control cultures [30]. We showed recently that MAP, in contrast to other closely related *M. avium* ssp., specifically suppressed the proinflammatory defense mechanisms of infected macrophages [31]. These results suggest that an insufficient TNF-α response in bovine paratuberculosis might favor mycobacterial persistence in macrophages and progression of disease.

In the present study, we show that reduced TNF-α transcript stability is responsible for lower TNF-α expression in MAP-infected macrophages. TNF-α transcript stability correlated with lower p38 MAPK activation in response to viable and heat-inactivated MAP as well as MAP-LM. These results provide evidence that the structural cell-wall composition of pathogenic mycobacteria restricts TNF-α expression in macrophages.

MATERIALS AND METHODS

Reagents

All chemicals were purchased from Sigma (Munich, Germany) unless otherwise stated. Mycobactin J was from Synbiotics (Stuttgart, Germany). LPS, purified from *Salmonella* Typhimurium (L6143), was obtained from Sigma. Actinomycin D and SB203580 were purchased from Calbiochem (Schwalbach, Germany). Oligonucleotide primers were obtained from MWG-Biotech (Ebersberg, Germany), [α^{32}P]-dCTP from Perkin-Elmer (Rodgau-Juegesheim, Germany), the phosphospecific anti-mouse p38 MAPK [pTpY$^{180/182}$] antibody from BioSource (Solingen, Germany), and the anti-mouse p38 MAPK antibody from New England Biolabs (Frankfurt, Germany).

Bacterial strains

The MAP strain DSM 44135 and the MS strain mc^{2}155 (ATCC 19420) were cultured and prepared for infection as described previously [32]. For some experiments, mycobacteria were inactivated by incubation for 15 min at 85°C as described [32].

Preparation of the LM from MAP and MS

LM preparations were performed according to the procedures of Chatterjee and coworkers [33–35], with some modifications. Briefly, the MAP strain 6783 was grown to confluence on Watson Reid medium (supplemented with Mycobactin J) in 600 ml tissue-culture flasks (6–12 weeks). The MS strain mc^{2}155 was conventionally grown in Middlebrook 7H9 broth to late log-phase (4 days). Bacteria were collected by centrifugation and washed with PBS (pH 7.5). Approximately 30 g (wet weight) was suspended in PBS containing 4% Triton X-114, protease inhibitor cocktail, DNaseI, and RNaseA (Sigma). The bacteria were disrupted by French Press, and lipids were extracted for 18 h at 4°C and overhead shaking. The insoluble material was removed by centrifugation for 1 h at 27,000 *g* at 4°C and was extracted subsequently with PBS containing 4% Triton X-114 extracts. The Triton X-114 extracts were combined, incubated at 37°C until biphasic partitioning, and centrifuged at 27,000 *g* for 30 min at 25°C. The detergent layer was collected, and macromolecules including LM were recovered by precipitation at –20°C with 95% ethanol (10 vol). The precipitates were suspended in endotoxin-free H_2O, and proteins were removed by phenol extraction. The material was dialyzed against H_2O. The crude carbohydrate mixture was fractionated by size-exclusion chromatography through Sephacryl S-200/S-100 columns (GE-Healthcare, Freiburg, Germany). Elution profiles were monitored by SDS-PAGE and silver-staining [36]. The LM-containing fractions were pooled and buffer contaminants removed by extensive dialysis against endotoxin-free H_2O. The solution was lyophilized, and the LM was resolved in endotoxin-free H_2O to a concentration of 1 mg/ml. Amounts of MAP- and MS-LM were visualized by SDS-PAGE, followed by periodic acid Schiff staining.

The endotoxin content of the preparations was controlled in the quality assurance department of IDT Biologika GmbH (Dessau-Rosslau, Germany) with a kinetic turbidimetric *Limulus* amoebocyte lysate assay (Charles River, Erkrath, Germany), according to the instructions of the European Pharmacopoeia (Ph. Eur. 2.6.14). The LM preparations contained insignificant amounts of endotoxin (≤0.2 EU/μg LM).

Macrophage cell culture and infection

The murine macrophage-like cell line RAW264.7 (ATCC, TIB-71) was maintained in complete medium [DMEM, supplemented with 10% (v/v) FCS, 1% (w/v) L-glutamine, 100 units/ml penicillin, and 100 μg/ml streptomycin, all from Invitrogen, Karlsruhe, Germany] at 37°C in the presence of 8% CO_2 in a humidified incubator. Infection of macrophages with mycobacteria and stimulation with LPS were performed as described [37]. Briefly, macrophages were incubated with a mycobacterial suspension of an indicated $OD_{660\ nm}$ in antibiotic-free medium for 2 h. Then, the medium was removed, and cells were washed with PBS and fed with fresh antibiotic-free medium. In some experiments, macrophages were stimulated with LPS (5 μg/ml) or with LM (0.25–4 μg/ml) and harvested at indicated timepoints.

In the titration experiments, macrophages were infected with mycobacteria by adding suspensions of $OD_{660\ nm}$ 0.2, 0.1, 0.05, 0.025, or 0.0125, representing MOI of ~20:1, 10:1, 5:1, 2.5:1, or 1:1, respectively, as described above.

For determination of mRNA-decay, macrophages were infected with mycobacteria or stimulated with LPS or LM for 2 h or 5 h and then

treated with actinomycin D (5 μg/ml) for up to 90 min. Where indicated, SB203580 (10 μM) was added simultaneously with actinomycin D.

Bacterial adhesion assay and flow cytometry

Adhesion of mycobacteria was assayed by flow cytometry as described previously [38] with some modifications. Briefly, mycobacteria were fluorescently labeled using PKH26 from Sigma. CFU (6×10^8) of bacteria were incubated in 5% glucose solution with 0.4% (v/v) PKH26 for 3 min. Excess dye was blocked by the addition of 1% FCS, and labeled bacteria were washed thoroughly before infection. To measure mycobacterial adhesion to RAW 264.7 macrophages, confluently grown cells were pretreated with cytochalasin D (3 μg/ml) for 30 min to inhibit phagocytosis and subsequently incubated with the indicated MOI of MAP and MS for 1 h. Then, bacteria-containing medium was removed, and cells were scraped off in PBS, washed for 5 min with PBS by overhead shaking at 4°C, and pelleted by centrifugation at 250 *g* for 5 min. Washing was repeated twice. Thereafter, the cells were analyzed with a BD FACSCalibur. Results are expressed as means ± SD of the mean fluorescence intensities.

RNA isolation and Northern analyses

Whole cell RNA was isolated using the RNeasy™ kit (Qiagen, Hilden, Germany), according to the manufacturer's instructions. Northern analyses were performed as described [39]. Hybridization was performed with [α^{32}P]-labeled plasmid DNA containing TNF-α and GAPDH cDNA fragments.

To illustrate differential mRNA decay and as TNF-α mRNA levels in MAP or MAP-LM-stimulated cells were much lower than in MS or in MS-LM-stimulated cells, in all mRNA stability experiments after hybridization with the TNF-α probe, the membranes from the MAP or MAP-LM groups were exposed longer to X-ray films to reach the TNF-α signal intensities of the MS or MS-LM groups. For detection of GAPDH mRNA as a loading control, equal exposure times were chosen to indicate that comparable amounts of mRNA from the MAP and MS macrophages were loaded on the membranes.

To quantify mRNA expression and decay, hybridization signals on X-ray films were scanned and digitally processed using the Imager MultiAnalyst (Bio-Rad, Hercules, CA, USA) for densitometric analyses. TNF-α signal intensities were normalized to the respective GAPDH signals from the same membrane. For each time-point of actinomycin D treatment, transcript abundance was referred to that obtained from macrophages at the time of actinomycin D addition, which was set to 100%. TNF-α mRNA half-life was calculated by regression analysis.

qRT-PCR and qPT-PCR

Before RT, 2 μg whole cell RNA was treated with DNaseI. cDNA was generated with random oligonucleotide primers and Superscript®II (Invitrogen), as described by the manufacturer. Identical samples from each group were processed in the absence of RT and served as controls for genomic DNA contamination. qRT-PCR was performed in a Mx3005P instrument (Stratagene, Heidelberg, Germany) using the oligonucleotide primers for *tnf* (5′-TACAGGCTTGTCACTCGAATT-3′, 5′-ATGAGCACAGAAAGCATGATC-3′) and *rps*9 (5′-TGACGTTGGCGGATGAGCACA-3′, 5′-CTGGACGAGGGCAAGATGAAGC-3′). PT-PCR was performed with oligonucleotide primer pairs recognizing the PTs of TNF-α as described by Murray [40]. Expression of *rps*9 served as control. For all PCR assays, 12.5 μl SYBR Green Supermix (Qiagen) was added to primers (final concentration, 250 nM) and cDNA in a total volume of 25 μl. The PCR conditions were 95°C for 10 min, 95°C for 20 s, 58°C for 30 s, and 72°C for 20 s, followed by a melting curve of the product as a control. Results were analyzed by the $2^{-(\Delta\Delta\text{comparative threshold})}$ method as described [41]. *rps*9 served as the control gene, and noninfected cells served as the calibrator.

ELISA analyses

TNF-α protein in cell culture supernatants was determined using an ELISA kit from R&D Systems (Wiesbaden-Nordenstadt, Germany), according to the manufacturer's instructions.

Protein extraction and immunoblot analyses

Confluent RAW264.7 cells were incubated with LPS or infected with mycobacteria as described above. After indicated time-points, cells were placed on ice, the medium was removed, and the cells were washed once with ice-cold PBS, and scraped in ice-cold PBS. Cells were collected after centrifugation for 15 s at 10,000 *g* and lysed in whole cell lysis buffer (10 mM Tris, pH 7.4, 30 mM $NaPP_i$, 50 mM NaCl, 1% Triton X-100, 2 mM Na_3VO_4, 50 mM sodium fluoride, and freshly added 0.5 mM PMSF, 0.5 μg/ml leupeptin, 0.5 μg/ml pepstatin, 10 mM *para*-nitrophenyl phosphate, 400 nM okadaic acid). After 10 min on ice, lysates were cleared by centrifugation for 15 min at 10,000 *g* and 4°C. Protein concentration of supernatants was determined by the Bradford method using Bio-Rad protein assay reagent, and samples were stored at −80°C. For immunoblot analyses, proteins (~50 μg) were separated by SDS-PAGE (10% acrylamide) and blotted onto polyvinylidene difluoride membranes (Millipore, Schwalbach, Germany). Equal loading and protein transfer were controlled by staining with Coomassie brilliant blue. Protein expression was detected by chemiluminescence with an alkaline-phosphatase-labeled secondary antibody.

RESULTS

TNF-α expression is weakly induced in MAP-infected macrophages

In paratuberculosis and other mycobacterial diseases, TNF-α expression at the sites of infection seems to be reduced through unknown mechanisms [29]. Macrophages are major TNF-α-producing cells, and several studies revealed that macrophages infected with pathogenic mycobacteria expressed lower TNF-α levels than macrophages infected with nonpathogenic mycobacteria [11–13, 42].

To gain more insights into the molecular mechanisms that contribute to TNF-α expression in MAP-infected macrophages, we first performed Northern analyses of TNF-α mRNA. Amounts of mRNA were compared in RAW264.7 macrophages infected with MAP or nonpathogenic MS or stimulated with LPS from *S.* Typhimurium (designated as MAP-macrophages, MS-macrophages, and LPS–macrophages, respectively). In the MS-macrophages, TNF-α mRNA expression was considerably higher than in MAP-macrophages at 2 h and 8 h after infection. The highest expression was observed in LPS-macrophages (**Fig. 1A**). Pretreatment of macrophages with cytochalasin D, a potent inhibitor of actin polymerization, did not influence differential TNF-α mRNA expression in mycobacteria-infected macrophages, indicating that it is not dependent on phagocytic uptake (data not shown). To analyze the molecular mechanisms underlying the different levels of TNF-α mRNA expression, we determined the amount of TNF-α primary RNA transcript as a parameter for transcriptional activation of the TNF-α gene and compared it with the levels of fully processed mRNA. Macrophages were stimulated with LPS or infected with MAP or MS. After 30 min, 2 h and 5 h RNA was isolated and analyzed by real-time qRT-PCR using an oligonucleotide primer pair that amplifies an exon-intron-overlapping cDNA fragment from the TNF-α PT [40] and an oligonucleotide

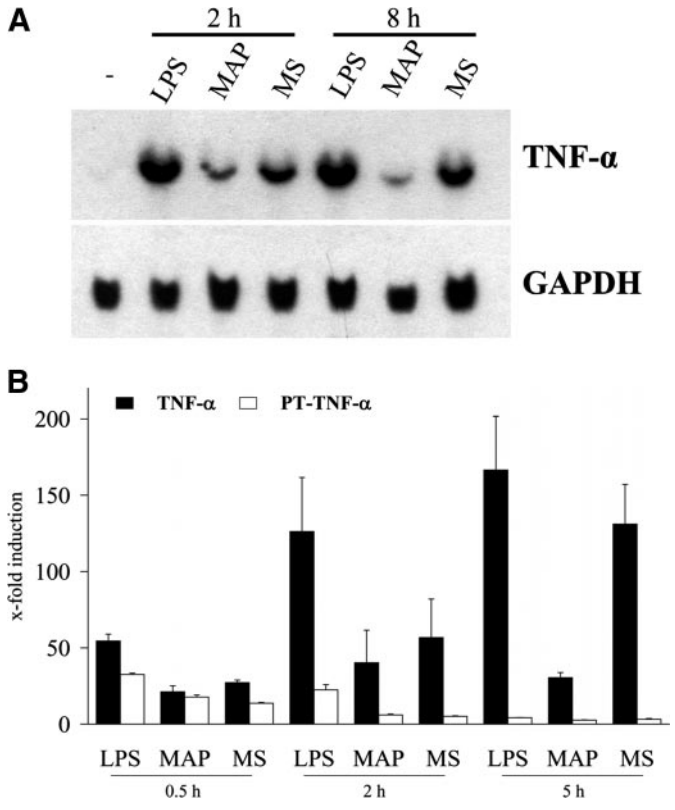

Figure 1. Differential TNF-α mRNA and PT expression kinetics in LPS-stimulated and MAP- or MS-infected macrophages. (A) Northern analyses of RAW264.7 cells infected with MAP or MS (MOI 10:1) or stimulated with LPS (5 μg/ml) as described in Materials and Methods. Cells were lysed at indicated time-points, and total RNA was isolated. Fifteen micrograms was separated by denaturating agarose gel electrophoresis, transferred onto nylon membranes, and subsequently hybridized with [α^{32}P]-labeled probes specific for TNF-α and GAPDH. The figure is representative of two experiments with similar results. (B) Total RNA was extracted from macrophages that had been stimulated with LPS or infected with MAP or MS (MOI 10:1) for 30 min, 2 h, and 5 h. After treatment with DNaseI, RNA was reverse-transcribed into cDNA with random oligonucleotide primers. qRT-PCR was performed with oligonucleotide primer pairs recognizing cDNA, obtained from TNF-α mRNA (TNF-α, solid bars) and from the PTs of TNF-α (PT-TNF-α, open bars). Results are given as fold changes of mRNA compared with untreated macrophages after normalization of each sample to *rps*9. Means ± SD of triplicates from one representative experiment of three are shown.

primer pair that amplifies an intron-spanning cDNA for TNF-α mRNA. As shown in Figure 1B, the amounts of the TNF-α primary RNA strongly increased after 30 min in LPS-macrophages, whereas the increase was approximately twofold lower and similar in MAP- and MS-macrophages. A similar expression pattern was observed after 2 h. After 5 h, levels of the TNF-α PT decreased in all groups to similar levels. At all times and in all groups, the amounts of TNF-α mRNA exceeded those of the PT, indicating that transcript stabilization occurred in LPS-, MAP-, and MS-macrophages. This effect was pronounced especially after 5 h when TNF-α PT expression was similar in all groups. However, although the decrease in PTs from 2 h to 5 h was associated with decreasing TNF-α mRNA levels in MAP-macrophages, the mRNA levels in LPS- and MS-macrophages increased, suggesting that the extent of TNF-α mRNA stabilization was considerably higher in LPS- and MS-macrophages than in MAP-macrophages.

Differences in TNF-α mRNA expression in LPS-stimulated and MAP- and MS-infected macrophages correlate with p38 MAPK activation

It has been shown that p38 MAPK signaling is involved in increased expression of TNF-α in LPS-stimulated macrophages. This is partially a result of a p38 MAPK-dependent stabilization of the TNF-α mRNA [26]. In addition, p38 MAPK signaling seems to be involved in induction of TNF-α expression in macrophages infected with MTB [43, 44]. Furthermore, diminished activation of p38 MAPK in primary bone marrow-derived macrophages was found after infection with pathogenic MAA as compared with macrophages infected with nonpathogenic MS [11, 13].

Therefore, we investigated p38 MAPK activation in cell lysates obtained from macrophages that were left untreated, stimulated with LPS, or infected with MAP or MS for the indicated times. Phosphorylation of p38 MAPK, as determined with a phospho-p38 MAPK-specific antibody, was maximally increased by LPS within 15 min and remained elevated for at least 120 min (**Fig. 2A**). Phosphorylation in response to MS at early time-points was less pronounced but similar to LPS at 60 min and 120 min. Phosphorylation in response to MAP was lowest at all time-points. The differences of p38 MAPK phosphorylation in MAP- and MS-macrophages were present for up to 8 h, however at much lower intensities (data not shown).

To analyze the differences of p38 MAPK phosphorylation in MAP- and MS-macrophages in more detail, we infected RAW264.7 macrophages with increasing amounts of MAP and MS and analyzed p38 MAPK phosphorylation after 30 min. As shown in Figure 2B, the amount of phosphorylated p38 MAPK in macrophages increased with increasing MOI of MAP, whereas in MS-infection, it reached a plateau at the second-lowest concentration tested. At each MOI, the magnitude of phosphorylation in MS-macrophages was higher than in MAP-macrophages. Lower phosphorylation levels of p38 MAPK in MAP-infected cells correlated with lower TNF-α mRNA and protein expression as determined by Northern blot and ELISA, respectively (Fig. 2, C and D). To rule out that a lower response of the cells to MAP was caused by decreased host-pathogen binding, adhesion assays were performed. At each MOI tested, adhesion of MAP to macrophages was markedly higher than of MS (Fig. 2E).

MAP-infected macrophages lack pronounced p38 MAPK-dependent TNF-α mRNA stability

To test if low p38 MAPK activation could account for a rapid degradation of TNF-α mRNA in MAP-infected cells, RAW264.7 macrophages were stimulated with LPS or infected with MAP or MS for 5 h. Then, decay kinetics of TNF-α mRNA was determined in the presence of actinomycin D, without or with addition of SB203580, a specific inhibitor of p38 MAPK. Based on the results

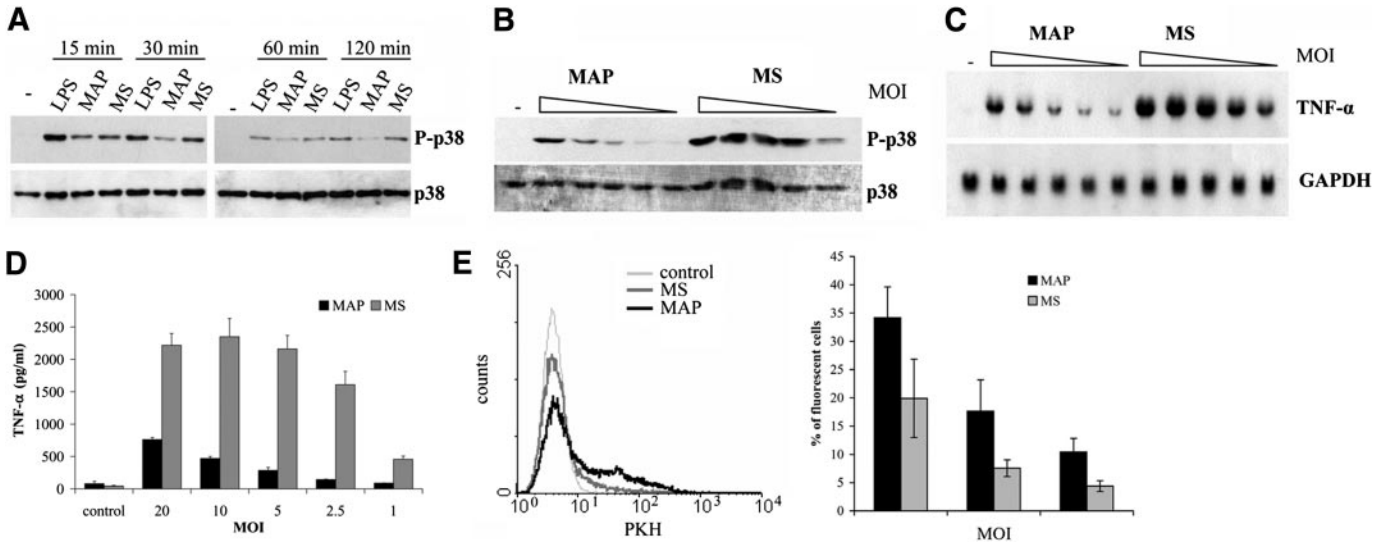

Figure 2. Differential activation of p38 MAPK in RAW264.7 cells stimulated with LPS or infected with MAP or MS correlates with differential TNF-α expression. (A) The amounts of p38 MAPK (p38) and phosphorylated p38 MAPK (P-p38) in RAW264.7 cells that had been infected with MAP or MS (MOI 10:1) or stimulated with LPS for indicated time-points were determined by immunoblotting using specific antibodies to phosphorylated and nonphosphorylated p38 MAPK. (B) The amount of p38 MAPK and phosphorylated p38 MAPK of RAW264.7 cells that had been infected with decreasing amounts of MAP or MS (MOI, from left to right 20:1, 10:1, 5:1, 2.5:1, 1:1) for 30 min was determined as in A. (C) RAW264.7 cells were infected with MAP or MS with indicated MOI for 6 h, and RNA was isolated for Northern analyses of TNF-α and GAPDH mRNAs as described in the legend to Figure 1. (A–C) Representative of at least two experiments with similar results. (D) Culture supernatants of RAW264.7 cells from the experiment shown in C were diluted 1:10 with PBS and analyzed for production of TNF-α by ELISA (means±SD of triplicates). Results were confirmed in two additional assays. (E) Flow cytometric analysis of adhesion of MAP and MS to RAW 264.7 macrophages. Cells treated with PKH26 (PKH)-labeled MAP or MS at a MOI of 20:1, 10:1, or 5:1 in the presence of cytochalasin D (3 μg/ml) were analyzed. At the left, a histogram of a representative experiment with labeled mycobacteria (PKH26) in a MOI of 10:1 is depicted. In the graph on the right, means ± SD of fluorescent cells relative to nonfluorescent cells from three independent experiments are shown.

shown in Figure 2, we performed mycobacterial infections at a MOI of 2.5:1, as at this MOI, clear differences in p38 MAPK were observed. As shown in **Figure 3A**, in LPS- and MS-macrophages, inhibition of p38 MAPK decreased TNF-α mRNA stability. SB203580 inhibited p38 MAPK in MAP-infected macrophages; however, inhibition was not as pronounced as in LPS- or-MS-macrophages. Densitometric analyses of this experiment revealed that the relative TNF-α transcript half-life was 40, 20, and 12 min in LPS-, MS-, and MAP-macrophages, respectively. In the presence of SB203580, we found a half-life of 14, 10, and 9 min in LPS-stimulated or MS- or MAP-macrophages, respectively. Similar results were obtained at different time-points (2 h or 8 h) and in experiments performed with higher MOI (10:1; data not shown). Thus, in MAP-macrophages, p38 MAPK-dependent TNF-α transcript stabilization occurred but to a much lesser extent than in LPS- and MS-macrophages. This suggested that p38 MAPK in MAP-macrophages was not activated sufficiently to confer substantial TNF-α mRNA stabilization, which resulted in lower TNF-α mRNA expression.

p38 MAPK activation and TNF-α mRNA stabilization are independent of mycobacterial viability

The structural components of the mycobacterial cell wall have been shown to induce TNF-α expression. In a previous study, we have shown that murine macrophages infected with viable and heat-inactivated MAP produce similar amounts of TNF-α [45], indicating that heat-stable mycobacterial structures might be responsible for its induction. Thus, we analyzed p38 MAPK phosphorylation and TNF-α mRNA transcript stability in RAW264.7 macrophages that were infected with viable and heat-inactivated MAP and MS. As shown in **Figure 4A**, after a 15-min treatment of the cells, p38 MAPK phosphorylation was similar in macrophages infected with viable (live) or heat-inactivated (dead) bacteria of MAP and MS. In agreement with the results shown in Figure 2A, live and dead MS induced stronger p38 MAPK phosphorylation than live and dead MAP.

Next, we determined TNF-α mRNA stability in RAW264.7 macrophages infected with heat-inactivated MAP and MS and compared it with that in macrophages infected with viable mycobacteria. Corresponding to the observations with live bacteria, TNF-α mRNA decay was faster in MAP-macrophages (Fig. 4B). These results indicated that differences in heat-stable mycobacterial components are responsible for different extents of p38 MAPK activation and TNF-α mRNA stabilization in MS- and MAP-macrophages.

MS-LM but not MAP-LM induces p38 MAPK-dependent TNF-α transcript stabilization

LAM and LM are heat-stable, integral components of the mycobacterial cell wall and are recognized by cells involved in the innate immune response [14]. In contrast to LAM, LM has been shown to induce strong TNF-α release in macrophages [15, 16]. Therefore, we extracted highly pure LM

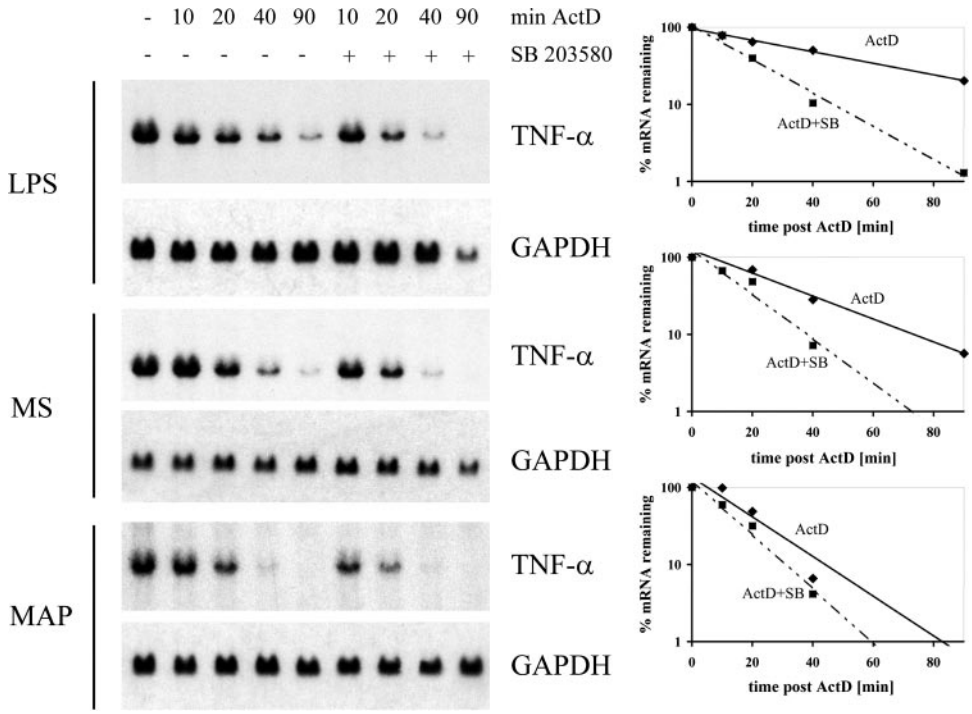

Figure 3. TNF-α mRNA stability in MS-infected macrophages but not in MAP-infected macrophages is decreased by p38 MAPK inhibition. RAW264.7 cells infected with MAP or MS (MOI 2.5:1) or stimulated with LPS (5 μg/ml) for 5 h (–) were subsequently treated with actinomycin D (ActD; 5 μg/ml), alone or with actinomycin D and 10 μM SB203580 for the indicated times. Total RNA was isolated, and Northern analysis for TNF-α and GAPDH mRNA was performed as described in the legend to Figure 1. Autoradiographs are shown on the left. For better comparison of TNF-α mRNA decay kinetics, the X-ray film for MAP-macrophages was exposed longer to obtain signal intensity similar to that for LPS- and MS-macrophages. Semi-logarithmic data demonstrating TNF-α mRNA decay kinetics obtained by the densitometric analysis of the autoradiographs are depicted on the right. Solid lines, Treatment with actinomycin D; broken lines, treatment with actinomycin D and SB203580 (ActD+SB). A representative experiment of at least two with similar results is shown.

from the MAP and MS strains of this study (**Fig. 5**) and used it for stimulation of RAW264.7 macrophages and analysis of TNF-α mRNA expression. As shown in **Figure 6A**, MAP- as well as MS-LM induced TNF-α mRNA expression in a concentration-dependent manner. Importantly, at each concentration, TNF-α mRNA expression was higher in MS-LM-treated than in MAP-LM-treated macrophages, which corresponded to the differences in TNF-α induction by whole bacteria (Fig. 2C). Next, we stimulated macrophages with 4 μg MS- or MAP-LM and analyzed TNF-α mRNA and TNF-α PT expression after 30 min and 2 h (Fig. 6B). At both times, TNF-α mRNA expression was induced after treatment with MS- or MAP-LM, but the induction of MS-LM was more pronounced and clearly exceeded that of MAP-LM-treated macrophages. The amounts of TNF-α PT induced by MS-LM exceeded that in MAP-LM-treated cells approximately four- and eightfold after 30 min and 2 h, respectively. The data in Figure 6B show that in MS-LM-treated macrophages, the amounts of TNF-α mRNA increased between 30 min and 2 h, whereas they remained constant in the MAP-LM-treated macrophages. On the other hand, PT levels decrease slightly in both cases. This suggests

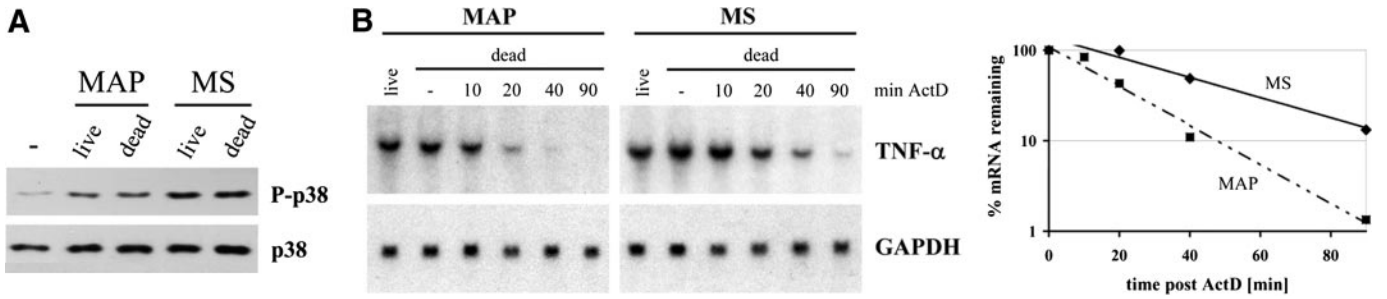

Figure 4. p38 MAPK activation and TNF-α mRNA stabilization are independent of mycobacterial viability. (A) RAW264.7 cells that had been treated with viable (live) or heat-inactivated (dead) MAP or MS (MOI 10:1) for 15 min were lysed and analyzed by immunoblotting using specific antibodies to phosphorylated and nonphosphorylated p38 MAPK. (B) RAW264.7 cells treated with heat-inactivated (dead) MAP or MS (MOI 10:1) for 2 h (–) were subsequently treated with actinomycin D (5 μg/ml) for the indicated times. For comparison, cells were infected with viable (live) MAP or MS for 2 h. Total RNA was isolated, and Northern analyses for TNF-α and GAPDH were performed as described in the legend to Figure 1. Autoradiographs are given on the left. For better comparison of TNF-α mRNA decay kinetics, the X-ray film for MAP-macrophages was exposed longer to obtain signal intensity similar to that for MS-macrophages. Semi-logarithmic data demonstrating TNF-α mRNA decay kinetics obtained by the densitometric analysis of the autoradiographs are depicted on the right. Broken line, Treatment with heat-inactivated MAP; solid line, treatment with heat-inactivated MS. The figure shows the results from a representative experiment of two.

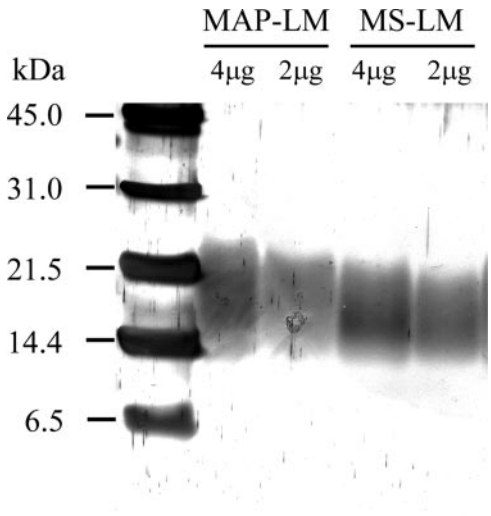

Figure 5. SDS-PAGE analysis of LM from MAP and MS. Similar amounts (2 μg/4 μg) of LM prepared from MAP (MAP-LM) and MS (MS-LM) were separated on a 15% SDS-PAGE gel and visualized by periodic acid silver-staining. Positions of molecular mass marker proteins are indicated.

that in MS-LM-treated macrophages, stability of the mRNA is higher as compared with the MAP-LM-treated cells.

As shown in Figure 6C, the amount of phosphorylated p38 MAPK in cells treated for 15 min with MS-LM exceeded that in cells treated with MAP-LM. To analyze TNF-α transcript stabilization in MS- and MAP-LM-treated macrophages, we determined the decay kinetics of TNF-α mRNA in the presence of actinomycin D, without or with addition of SB203580 mRNA. As shown in Figure 6D, left, in MAP-LM-treated macrophages, TNF-α mRNA stability was significantly lower than in MS-LM-treated macrophages and was not influenced by SB203580. For MS-LM-treated cells, densitometric analysis (Fig. 6D, right) revealed a TNF-α transcript half-life of 26 min, which was reduced to 12 min in the presence of SB203580. In contrast, in MAP-LM-treated macrophages, TNF-α transcript half-lives of 9 min and 8 min were obtained in the absence and presence of SB203580, respectively. Thus, MAP-LM-induced p38 MAPK activation seemed not to be sufficient to induce TNF-α transcript stabilization.

In summary, these data indicate that the LM of pathogenic and nonpathogenic mycobacteria seems to be involved in the induction of TNF-α mRNA expression. The LM of nonpathogenic MS, however, is the more potent activator of p38 MAPK, which leads to increased TNF-α transcript stabilization and TNF-α mRNA expression as compared with macrophages treated with the LM from pathogenic MAP.

DISCUSSION

TNF-α is considered a key factor for host control of mycobacterial infection, as underlined by the findings that it can inhibit mycobacterial growth in vitro, TNF-α-deficient mice are more susceptible to aerosol MTB infection, and anti-TNF-α treatment of individuals latently infected with MTB exacerbates disease [6]. Several lines of evidence indicate that TNF-α production in mycobacterial diseases is insufficient and that this might favor persistence of mycobacteria [9–13]. Correspondingly, in bovine paratuberculosis, TNF-α expression seems to be reduced at sites of MAP infection [29]. As macrophages are major TNF-α producers and likewise, are the target cells of mycobacterial survival, it is plausible to assume that pathogenic mycobacteria subvert regulatory mechanisms in macrophages affecting TNF-α expression.

In the present study, we provide evidence that macrophages infected with pathogenic MAP, compared with macrophages stimulated with LPS or infected with nonpathogenic MS, exhibit reduced TNF-α mRNA and protein expression. We could show that these differences resulted, to a large extent, from different p38 MAPK-dependent TNF-α mRNA stabilization. Furthermore, our results suggest that these differences were caused, at least in part, by differences in the properties of LM, heat-stable cell-surface components, which can trigger TNF-α formation. LM of MAP induced only low levels of TNF-α and activation of p38 MAPK as compared with LM of the nonpathogenic MS.

As a model of TNF-α regulation in mycobacteria-infected macrophages, we used the murine RAW264.7 macrophage cell line, which has been used extensively to study mechanisms controlling TNF-α expression [23, 24, 26, 46, 47]. Thus, it has been shown that strong induction of TNF-α mRNA by LPS involved increased transcription of the TNF-α gene as well as stabilization of TNF-α mRNA [24, 48]. We could show that transcriptional activation and post-transcriptional p38 MAPK-independent mRNA stabilization contribute to differential gene expression of the immune-responsive gene *irg*1 in LPS-, MS-, and MAP-macrophages [37].

In contrast to pathogenic MAP, nonpathogenic MS did not survive in murine macrophages and did not inhibit phagosomal acidification and phagosome-lysosome fusion [32]. In the present study, we observed lower TNF-α mRNA expression in RAW264.7 macrophages infected with MAP than in cells infected with MS or activated by LPS (Fig. 1). Transcriptional initiation of the TNF-α gene serves as the primary control point of the regulation of TNF-α production [20, 21, 49], and it is proposed that stimulation with LPS and MTB may recruit the same "enhanceosome" to the TNF-α promoter region [50]. Determination of TNF-α PT levels as a parameter for transcription revealed two- and fourfold higher expression in LPS-stimulated than in mycobacteria-infected macrophages after 30 min and 2 h, respectively. There was no significant difference after 5 h. Interestingly, no major differences in transcription were found between MAP- and MS-macrophages. Therefore, the differences in TNF-α mRNA expression shown by Northern and RT-PCR (Fig. 1) should result, to a major extent, from TNF-α mRNA stabilization, which we confirmed with the experiments shown in Figure 3. Thus, lower TNF-α expression in MAP-macrophages was accompanied by lower mRNA stability.

Studies with specific inhibitors have indicated that MAPK signaling is essential for TNF-α expression in LPS-stimulated macrophages [51]. p38 MAPK is implicated in macrophage

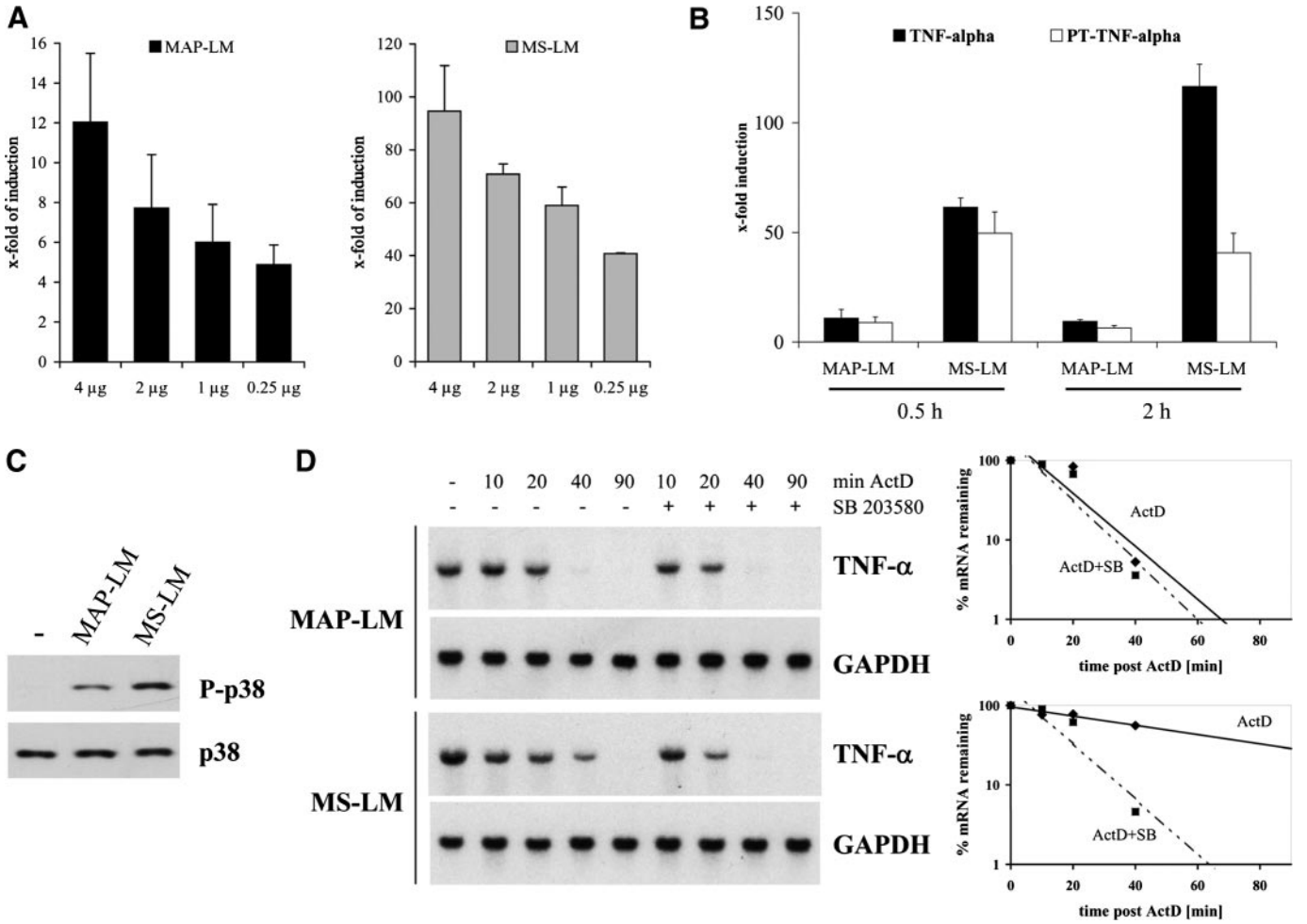

Figure 6. MS-LM induces p38 MAPK-dependent TNF-α transcript stabilization. (A) qRT-PCR of TNF-α gene expression in macrophages treated for 2 h with increasing amounts of MAP (solid bars)- and MS (shaded bars)-LM. Means of triplicates from one representative experiment of three are shown. Results are given as fold changes of mRNA compared with untreated macrophages after normalization of each sample to *rps*9. (B) Total RNA was extracted from macrophages that had been stimulated with 4 µg/ml MAP- or MS-LM for 30 min and 2 h. qRT-PCR for TNF-α mRNA (TNF-α, solid bars) and the PTs of TNF-α (PT-TNF-α, open bars) were performed as described for Figure 1. Results are given as fold changes of mRNA compared with untreated macrophages after normalization of each sample to *rps*9. Means of the triplicates from one out of three experiments with similar results are shown. (C) RAW264.7 cells that had been treated without or with 4 µg/ml MAP- or MS-LM for 30 min were lysed and analyzed by immunoblotting using specific antibodies to phosphorylated and nonphosphorylated p38 MAPK. (D) RAW264.7 cells were stimulated with 4 µg/ml MAP- or MS-LM for 2 h (–), and then, macrophages were treated with actinomycin D (5 µg/ml) or with actinomycin D and 10 µM SB203580 for the indicated times. Total RNA was isolated and Northern analyses for TNF-α and GAPDH performed as described in the legend of Figure 1. Autoradiographs are shown on the left. For better comparison of TNF-α mRNA decay kinetics, the X-ray film for MAP-LM-treated macrophages was exposed longer to obtain signal intensity similar to that for MS-LM-treated macrophages. Semi-logarithmic data demonstrating TNF-α mRNA decay kinetics obtained by the densitometric analysis of the autoradiographs are depicted on the right. Solid lines, Treatment with actinomycin D; broken lines, treatment with actinomycin D and SB203580. (C and D) Representative of at least two experiments with similar results.

signaling, leading to LPS-induced mRNA stabilization [26]. There is evidence that p38 MAPK signaling also contributes to TNF-α expression in mycobacteria-infected macrophages [43, 44]. Furthermore, low TNF-α expression in MAA- as compared with MS-infected primary bone marrow-derived macrophages has been attributed to diminished activation of p38 MAPK in MAA-infected cells [11–13, 42]. We found that the lower TNF-α mRNA expression in MAP-macrophages, as compared with MS-macrophages, correlated with lower p38 MAPK activation by MAP (Fig. 2).

The enzyme activity of p38 MAPK is reversibly inhibited by pyridinyl imidazole compounds such as SB203580, which compete with ATP for access to the catalytic site [52]. SB203580 does not affect TNF-α mRNA transcription in RAW264.7 macrophages [53]. To clarify the role of active p38 MAPK for TNF-α mRNA stability in mycobacteria-infected macrophages, TNF-α mRNA decay was monitored in the absence or presence of SB203580 5 h after infection or stimulation with LPS. In agreement with Brook et al. [26], TNF-α mRNA in LPS-macrophages was degraded more rapidly upon inhibition of p38

MAPK (Fig. 3). Similar results were obtained for MS-macrophages, indicating a central role of p38 MAPK for TNF-α transcript stability, also in mycobacteria-infected macrophages. However, only a weak increase in the rapid degradation of TNF-α mRNA in MAP-macrophages could be detected (Fig. 3).

Based on our results, we conclude that p38 MAPK activation is critical for TNF-α mRNA expression in mycobacteria-infected macrophages. Lower TNF-α production in MAP-macrophages than in MS-macrophages can be attributed to low p38 MAPK activation, which is insufficient to increase stability of the TNF-α mRNA to an extent that elevates TNF-α expression substantially. However, the precise mechanisms of p38 MAPK-dependent regulation of TNF-α mRNA stability are still incompletely understood. A major role is played by the p38 MAPK downstream target MK2. Mice deficient in MK2 exhibit impaired production of TNF-α [54]. p38 MAPK and MK2 control the expression and function of tristetraprolin [55–57], which destabilizes TNF-α mRNA through interaction with its ARE. The TNF-α ARE also interacts with the destabilizing protein, KH-type splicing regulatory protein, which is phosphorylated by p38 MAPK itself, leading to mRNA stabilization [58]. In addition, other ARE-binding proteins might be involved.

The mechanism of how pathogenic mycobacteria manage to circumvent TNF-α induction is still unclear. Several biological effects of mycobacteria on their host cells depend on the viability of the mycobacteria. For example, only viable MAP is able to inhibit phagosomal maturation [32]. Furthermore, it has been shown that MAP expresses an active phosphatase, which was identified in the cytosol of infected macrophages, where it could probably interfere with signaling processes [59]. In addition, we showed that the antigen-specific stimulatory capacity of murine macrophages for a $CD4^+$ T cell line was inhibited significantly after infection with viable but not with heat-inactivated MAP; however, the production of TNF-α was similar [45]. The latter result prompted us to analyze whether mycobacterial viability had an effect on p38 MAPK activation and TNF-α transcript stabilization. In agreement with results obtained with macrophages infected with viable MAP or MS, macrophages infected with heat-inactivated mycobacteria also displayed the typical mycobacteria-dependent p38 MAPK activation and TNF-α transcript stabilization profile (Fig. 4). This indicated that heat-stable surface components of the mycobacteria mediate the TNF-α mRNA expression and the differences in TNF-α mRNA expression.

Two of the most abundant heat-stable components of the mycobacterial cell wall are the lipoglycans LAM and LM [60]. These structures are expressed on the mycobacterial cell surface [61] and can induce granuloma formation [62]. The biological activities of these lipoglycans depend on their structural features [15, 16, 63]. LM is composed of a phosphatidyl-myo-inositol anchor, which is polymannosylated to different degrees, according to the mycobacterial species, the so-called D-mannan core [60]. LAM corresponds to LM, in which the D-mannan core is supplemented further with a D-arabinan domain [60]. Depending on the mycobacterial species, the nonreducing termini of the D-arabinan domain can be capped with phosphatidyl-myo-inositol units (PILAM) or with oligomannosyl units (ManLAM), such as in nonpathogenic mycobacteria and pathogenic mycobacteria, respectively [64–67]. The terminal phosphatidyl-myo-inositol caps enable PILAM to induce TNF-α expression of macrophages, whereas ManLAM has only little TNF-α-inducing capacity, which has been attributed to its terminal mannose caps. The LM of pathogenic and nonpathogenic mycobacteria has been shown to induce TNF-α release in macrophages [15, 16, 63]. However, the TNF-α-inducing activity differs between different LM and seemed to be determined directly by their D-mannan core length [63].

Here, we demonstrated that MAP-LM and MS-LM induced TNF-α mRNA expression in RAW264.7 macrophages in a concentration-dependent manner (Fig. 6). MS-LM, at low concentration, already induced considerably higher amounts of TNF-α mRNA than MAP-LM. Similar results were obtained in experiments performed in the presence of polymyxin B to exclude LPS contamination (data not shown). The most interesting finding was that in macrophages treated with MAP-LM, the amounts of TNF-α mRNA were only slightly higher than that of the PT, which was associated with weak p38 MAPK activation, whereas in macrophages treated with MS-LM, the amounts of TNF-α mRNA clearly exceeded those of the PTs. This correlated with a higher p38 MAPK activation and TNF-α mRNA stabilization. These results indicate that in MAP-LM-treated macrophages, p38 MAPK activation is insufficient to induce transcript stabilization and increase TNF-α mRNA levels. Different TNF-α transcript stabilization by LM from different mycobacterial species has not yet been reported. Whether this may result from a different D-mannan core length or other structural differences awaits further studies.

Little is known about the receptors that mediate LM-induced signals in macrophages. As stated above, LM from different mycobacterial species has been shown to induce TNF-α production to a similar extent. Thus, comparable amounts of TNF-α were produced by macrophages stimulated with LM from *Mycobacterium chelonae*, *Mycobacterium kansasii*, or MS. A CD14-TLR2-MyD88-dependent mechanism has been postulated for this [15, 16]. It appears likely that this pathway is involved in MAP-LM-induced TNF-α expression. The lower TNF-α production in MAP-LM compared with MS-LM-stimulated macrophages, however, indicates that other receptors, most likely recognizing structural differences in the LM, might be involved.

In conclusion, our results suggest that the structural features of pathogenic mycobacteria lead to insufficient activation of p38 MAPK and a higher TNF-α mRNA turnover and as a consequence, to lower TNF-α expression, as compared with nonpathogenic mycobacteria. The impact of the described mechanism on mycobacterial survival and virulence needs to be elucidated in future studies.

ACKNOWLEDGMENTS

This work was supported by the Deutsche Forschungsgemeinschaft (Bonn, Germany) Grants SFB621 to P. V-W. and R. G., SFB566 to H. H., and Go983/1 to R. G. and a grant of the Germany Ministry for Science and Education to R. G. (BMBF,

01KI0750). We are grateful to Sabine Goebel, Kristin Laarmann, and Julian Sander for their excellent technical assistance, to Maren Seitz for the help in flow cytometric analyses, and to Joerg Merkel for excellent computer technical support. We thank Prof. Dr. H-J. Selbitz (IDT Biologika GmbH, Germany) for endotoxin determination. Finally, we thank Prof. Alan Rowe Schenkel (Colorado State University, Ft. Collins, CO, USA) for critical reading of the manuscript.

REFERENCES

1. Kaneko, H., Yamada, H., Mizuno, S., Udagawa, T., Kazumi, Y., Sekikawa, K., Sugawara, I. (1999) Role of tumor necrosis factor-α in *Mycobacterium*-induced granuloma formation in tumor necrosis factor-α-deficient mice. *Lab. Invest.* **79,** 379–386.
2. Cosma, C. L., Sherman, D. R., Ramakrishnan, L. (2003) The secret lives of the pathogenic mycobacteria. *Annu. Rev. Microbiol.* **57,** 641–676.
3. Clarke, C. J. (1997) The pathology and pathogenesis of paratuberculosis in ruminants and other species. *J. Comp. Pathol.* **116,** 217–261.
4. Beutler, B., Cerami, A. (1989) The biology of cachectin/TNF—a primary mediator of the host response. *Annu. Rev. Immunol.* **7,** 625–655.
5. Feldmann, M., Brennan, F. M., Maini, R. N. (1996) Role of cytokines in rheumatoid arthritis. *Annu. Rev. Immunol.* **14,** 397–440.
6. Stenger, S. (2005) Immunological control of tuberculosis: role of tumor necrosis factor and more. *Ann. Rheum. Dis.* **64** (Suppl. 4), iv24–iv28.
7. Bermudez, L. E., Young, L. S. (1990) Killing of *Mycobacterium avium*: insights provided by the use of recombinant cytokines. *Res. Microbiol.* **141,** 241–243.
8. Bermudez, L. E., Young, L. S. (1988) Tumor necrosis factor, alone or in combination with IL-2, but not IFN-γ, is associated with macrophage killing of *Mycobacterium avium* complex. *J. Immunol.* **140,** 3006–3013.
9. Falcone, V., Bassey, E. B., Toniolo, A., Conaldi, P. G., Collins, F. M. (1994) Differential release of tumor necrosis factor-α from murine peritoneal macrophages stimulated with virulent and avirulent species of mycobacteria. *FEMS Immunol. Med. Microbiol.* **8,** 225–232.
10. Beltan, E., Horgen, L., Rastogi, N. (2000) Secretion of cytokines by human macrophages upon infection by pathogenic and non-pathogenic mycobacteria. *Microb. Pathog.* **28,** 313–318.
11. Yadav, M., Roach, S. K., Schorey, J. S. (2004) Increased mitogen-activated protein kinase activity and TNF-α production associated with *Mycobacterium smegmatis*- but not *Mycobacterium avium*-infected macrophages requires prolonged stimulation of the calmodulin/calmodulin kinase and cyclic AMP/protein kinase A pathways. *J. Immunol.* **172,** 5588–5597.
12. Lee, S. B., Schorey, J. S. (2005) Activation and mitogen-activated protein kinase regulation of transcription factors Ets and NF-κB in *Mycobacterium*-infected macrophages and role of these factors in tumor necrosis factor α and nitric oxide synthase 2 promoter function. *Infect. Immun.* **73,** 6499–6507.
13. Roach, S. K., Schorey, J. S. (2002) Differential regulation of the mitogen-activated protein kinases by pathogenic and nonpathogenic mycobacteria. *Infect. Immun.* **70,** 3040–3052.
14. Briken, V., Porcelli, S. A., Besra, G. S., Kremer, L. (2004) Mycobacterial lipoarabinomannan and related lipoglycans: from biogenesis to modulation of the immune response. *Mol. Microbiol.* **53,** 391–403.
15. Vignal, C., Guerardel, Y., Kremer, L., Guérardel, Y., Nigou, J., Puzo, G., Erard, F., Ryffel, B. (2003) Lipomannans, but not lipoarabinomannans, purified from *Mycobacterium chelonae* and *Mycobacterium kansasii* induce TNF-α and IL-8 secretion by a CD14-Toll-like receptor 2-dependent mechanism. *J. Immunol.* **171,** 2014–2023.
16. Quesniaux, V. J., Nicolle, D. M., Torres, D., Kremer, L., Guérardel, Y., Nigou, J., Puzo, G., Erard, F., Ryffel, B. (2004) Toll-like receptor 2 (TLR2)-dependent-positive and TLR2-independent-negative regulation of proinflammatory cytokines by mycobacterial lipomannans. *J. Immunol.* **172,** 4425–4434.
17. Drouet, C., Shakhov, A. N., Jongeneel, C. V. (1991) Enhancers and transcription factors controlling the inducibility of the tumor necrosis factor-α promoter in primary macrophages. *J. Immunol.* **147,** 1694–1700.
18. Kim, Y. M., Lee, B. S., Yi, K. Y., Paik, S. G. (1997) Upstream NF-κB site is required for the maximal expression of mouse inducible nitric oxide synthase gene in interferon-γ plus lipopolysaccharide-induced RAW 264.7 macrophages. *Biochem. Biophys. Res. Commun.* **236,** 655–660.
19. Lieberman, A. P., Pitha, P. M., Shin, M. L. (1992) Poly(A) removal is the kinase-regulated step in tumor necrosis factor mRNA decay. *J. Biol. Chem.* **267,** 2123–2126.
20. Falvo, J. V., Uglialoro, A. M., Brinkman, B. M., Merika, M., Parekh, B. S., Tsai, E. Y., King, H. C., Morielli, A. D., Peralta, E. G., Maniatis, T., Thanos, D., Goldfeld, A. E. (2000) Stimulus-specific assembly of enhancer complexes on the tumor necrosis factor α gene promoter. *Mol. Cell. Biol.* **20,** 2239–2247.
21. Tsai, E. Y., Falvo, J. V., Tsytsykova, A. V., Barczak, A. K., Reimold, A. M., Glimcher, L. H., Fenton, M. J., Gordon, D. C., Dunn, I. F., Goldfeld, A. E. (2000) A lipopolysaccharide-specific enhancer complex involving Ets, Elk-1, Sp1, and CREB binding protein and p300 is recruited to the tumor necrosis factor α promoter in vivo. *Mol. Cell. Biol.* **20,** 6084–6094.
22. Kontoyiannis, D., Pasparakis, M., Pizarro, T. T., Cominelli, F., Kollias, G. (1999) Impaired on/off regulation of TNF biosynthesis in mice lacking TNF AU-rich elements: implications for joint and gut-associated immunopathologies. *Immunity* **10,** 387–398.
23. Anderson, P., Phillips, K., Stoecklin, G., Kedersha, N. (2004) Post-transcriptional regulation of proinflammatory proteins. *J. Leukoc. Biol.* **76,** 42–47.
24. Han, J. H., Beutler, B., Huez, G. (1991) Complex regulation of tumor necrosis factor mRNA turnover in lipopolysaccharide-activated macrophages. *Biochim. Biophys. Acta* **1090,** 22–28.
25. Dean, J. L., Sully, G., Clark, A. R., Saklatvala, J. (2004) The involvement of AU-rich element-binding proteins in p38 mitogen-activated protein kinase pathway-mediated mRNA stabilization. *Cell. Signal.* **16,** 1113–1121.
26. Brook, M., Sully, G., Clark, A. R., Saklatvala, J. (2000) Regulation of tumor necrosis factor α mRNA stability by the mitogen-activated protein kinase p38 signaling cascade. *FEBS Lett.* **483,** 57–61.
27. Grant, I. R., Williams, A. G., Rowe, M. T., Muir, D. D. (2005) Efficacy of various pasteurization time-temperature conditions in combination with homogenization on inactivation of *Mycobacterium avium* subsp. *paratuberculosis* in milk. *Appl. Environ. Microbiol.* **71,** 2853–2861.
28. Harris, N. B., Barletta, R. G. (2001) *Mycobacterium avium* subsp. *paratuberculosis* in veterinary medicine. *Clin. Microbiol. Rev.* **14,** 489–512.
29. Coussens, P. M. (2004) Model for immune responses to *Mycobacterium avium* subspecies *paratuberculosis* in cattle. *Infect. Immun.* **72,** 3089–3096.
30. Weiss, D. J., Evanson, O. A., Moritz, A., Deng, M. Q., Abrahamsen, M. S. (2002) Differential responses of bovine macrophages to *Mycobacterium avium* subsp. *paratuberculosis* and *Mycobacterium avium* subsp. *avium*. *Infect. Immun.* **70,** 5556–5561.
31. Basler, T., Geffers, R., Weiss, S., Valentin-Weigand, P., Goethe, R. (2008) *Mycobacterium avium* subspecies induce differential expression of pro-inflammatory mediators in a murine macrophage model: evidence for enhanced pathogenicity of *Mycobacterium avium* subspecies *paratuberculosis*. *Immunobiology* **213,** 879–888.
32. Kuehnel, M. P., Goethe, R., Habermann, A., Mueller, E., Rohde, M., Griffiths, G., Valentin-Weigand, P. (2001) Characterization of the intracellular survival of *Mycobacterium avium* ssp. *paratuberculosis*: phagosomal pH and fusogenicity in J774 macrophages compared with other mycobacteria. *Cell. Microbiol.* **3,** 551–566.
33. Chatterjee, D., Hunter, S. W., McNeil, M., Brennan, P. J. (1992) Lipoarabinomannan. Multiglycosylated form of the mycobacterial mannosylphosphatidylinositols. *J. Biol. Chem.* **267,** 6228–6233.
34. Chatterjee, D., Roberts, A. D., Lowell, K., Brennan, P. J., Orme, I. M. (1992) Structural basis of capacity of lipoarabinomannan to induce secretion of tumor necrosis factor. *Infect. Immun.* **60,** 1249–1253.
35. Khoo, K. H., Douglas, E., Azadi, P., Inamine, J. M., Besra, G. S., Mikusová, K., Brennan, P. J., Chatterjee, D. (1996) Truncated structural variants of lipoarabinomannan in ethambutol drug-resistant strains of *Mycobacterium smegmatis*. Inhibition of arabinan biosynthesis by ethambutol. *J. Biol. Chem.* **271,** 28682–28690.
36. Tsai, C. M., Frasch, C. E. (1982) A sensitive silver stain for detecting lipopolysaccharides in polyacrylamide gels. *Anal. Biochem.* **119,** 115–119.
37. Basler, T., Jeckstadt, S., Valentin-Weigand, P., Goethe, R. (2006) *Mycobacterium paratuberculosis*, *Mycobacterium smegmatis*, and lipopolysaccharide induce different transcriptional and post-transcriptional regulation of the IRG1 gene in murine macrophages. *J. Leukoc. Biol.* **79,** 628–638.
38. Pott, J., Basler, T., Duerr, C. U., Rohde, M., Goethe, R., Hornef, M. W. (2009) Internalization-dependent recognition of *Mycobacterium avium* ssp. *paratuberculosis* by intestinal epithelial cells. *Cell. Microbiol.*, Epub ahead of print.
39. Goethe, R., Phi-van, L. (1998) Posttranscriptional lipopolysaccharide regulation of the lysozyme gene at processing of the primary transcript in myelomonocytic HD11 cells. *J. Immunol.* **160,** 4970–4978.
40. Murray, P. J. (2005) The primary mechanism of the IL-10-regulated anti-inflammatory response is to selectively inhibit transcription. *Proc. Natl. Acad. Sci. USA* **102,** 8686–8691.
41. Livak, K. J., Schmittgen, T. D. (2001) Analysis of relative gene expression data using real-time quantitative PCR and the 2(–Δ Δ C(T)) method. *Methods* **25,** 402–408.
42. Yadav, M., Clark, L., Schorey, J. S. (2006) Macrophage's proinflammatory response to a mycobacterial infection is dependent on sphingosine kinase-mediated activation of phosphatidylinositol phospholipase C, protein kinase C, ERK1/2, and phosphatidylinositol 3-kinase. *J. Immunol.* **176,** 5494–5503.
43. Surewicz, K., Aung, H., Kanost, R. A., Jones, L., Hejal, R., Toossi, Z. (2004) The differential interaction of p38 MAP kinase and tumor necrosis factor-α in human alveolar macrophages and monocytes induced by *Mycobacterium tuberculois*. *Cell. Immunol.* **228,** 34–41.
44. Song, C. H., Lee, J. S., Lee, S. H., Lim, K., Kim, H. J., Park, J. K., Paik, T. H., Jo, E. K. (2003) Role of mitogen-activated protein kinase pathways in the production of tumor necrosis factor-α, interleukin-10, and mono-

cyte chemotactic protein-1 by *Mycobacterium tuberculosis* H37Rv-infected human monocytes. *J. Clin. Immunol.* **23,** 194–201.
45. Zur Lage, S., Goethe, R., Darji, A., Valentin-Weigand, P., Weiss, S. (2003) Activation of macrophages and interference with CD4+ T-cell stimulation by *Mycobacterium avium* subspecies *paratuberculosis* and *Mycobacterium avium* subspecies *avium*. *Immunology* **108,** 62–69.
46. Han, J., Brown, T., Beutler, B. (1990) Endotoxin-responsive sequences control cachectin/tumor necrosis factor biosynthesis at the translational level. *J. Exp. Med.* **171,** 465–475.
47. Han, J., Beutler, B. (1990) The essential role of the UA-rich sequence in endotoxin-induced cachectin/TNF synthesis. *Eur. Cytokine Netw.* **1,** 71–75.
48. Beutler, B., Cerami, A. (1988) Tumor necrosis, cachexia, shock, and inflammation: a common mediator. *Annu. Rev. Biochem.* **57,** 505–518.
49. Goldfeld, A. E., Maniatis, T. (1989) Coordinate viral induction of tumor necrosis factor α and interferon β in human B cells and monocytes. *Proc. Natl. Acad. Sci. USA* **86,** 1490–1494.
50. Barthel, R., Tsytsykova, A. V., Barczak, A. K., Tsai, E. Y., Dascher, C. C., Brenner, M. B., Goldfeld, A. E. (2003) Regulation of tumor necrosis factor α gene expression by mycobacteria involves the assembly of a unique enhanceosome dependent on the coactivator proteins CBP/p300. *Mol. Cell. Biol.* **23,** 526–533.
51. Zhu, W., Downey, J. S., Gu, J., Di Padova, F., Gram, H., Han, J. (2000) Regulation of TNF expression by multiple mitogen-activated protein kinase pathways. *J. Immunol.* **164,** 6349–6358.
52. Young, P. R., McLaughlin, M. M., Kumar, S., Kassis, S., Doyle, M. L., McNulty, D., Gallagher, T. F., Fisher, S., McDonnell, P. C., Carr, S. A., Huddleston, M. J., Seibel, G., Porter, T. G., Livi, G. P., Adams, J. L., Lee, J. C. (1997) Pyridinyl imidazole inhibitors of p38 mitogen-activated protein kinase bind in the ATP site. *J. Biol. Chem.* **272,** 12116–12121.
53. Baldassare, J. J., Bi, Y., Bellone, C. J. (1999) The role of p38 mitogen-activated protein kinase in IL-1 β transcription. *J. Immunol.* **162,** 5367–5373.
54. Kotlyarov, A., Neininger, A., Schubert, C., Eckert, R., Birchmeier, C., Volk, H. D., Gaestel, M. (1999) MAPKAP kinase 2 is essential for LPS-induced TNF-α biosynthesis. *Nat. Cell Biol.* **1,** 94–97.
55. Mahtani, K. R., Brook, M., Dean, J. L., Sully, G., Saklatvala, J., Clark, A. R. (2001) Mitogen-activated protein kinase p38 controls the expression and posttranslational modification of tristetraprolin, a regulator of tumor necrosis factor α mRNA stability. *Mol. Cell. Biol.* **21,** 6461–6469.
56. Stoecklin, G., Stubbs, T., Kedersha, N., Wax, S., Rigby, W. F., Blackwell, T. K., Anderson, P. (2004) MK2-induced tristetraprolin:14-3-3 complexes prevent stress granule association and ARE-mRNA decay. *EMBO J.* **23,** 1313–1324.
57. Hitti, E., Iakovleva, T., Brook, M., Deppenmeier, S., Gruber, A. D., Radzioch, D., Clark, A. R., Blackshear, P.J ,. Kotlyarov, A., Gaestel, M. (2006) Mitogen-activated protein kinase-activated protein kinase 2 regulates tumor necrosis factor mRNA stability and translation mainly by altering tristetraprolin expression, stability, and binding to adenine/uridine-rich element. *Mol. Cell. Biol.* **26,** 2399–2407.
58. Briata, P., Forcales, S. V., Ponassi, M., Corte, G., Chen, C. Y., Karin, M., Puri, P. L., Gherzi, R. (2005) p38-Dependent phosphorylation of the mRNA decay-promoting factor KSRP controls the stability of select myogenic transcripts. *Mol. Cell* **20,** 891–903.
59. Bach, H., Sun, J., Hmama, Z., Av-Gay, Y. (2006) *Mycobacterium avium* subsp. *paratuberculosis* PtpA is an endogenous tyrosine phosphatase secreted during infection. *Infect. Immun.* **74,** 6540–6546.
60. Chatterjee, D. (1997) The mycobacterial cell wall: structure, biosynthesis and sites of drug action. *Curr. Opin. Chem. Biol.* **1,** 579–588.
61. Pitarque, S., Larrouy-Maumus, G., Payre, B., Jackson, M., Puzo, G., Nigou, J. (2008) The immunomodulatory lipoglycans, lipoarabinomannan and lipomannan, are exposed at the mycobacterial cell surface. *Tuberculosis (Edinb.)* **88,** 560–565.
62. Puissegur, M. P., Lay, G., Gilleron, M., Botella, L., Nigou, J., Marrakchi, H., Mari, B., Duteyrat, J. L., Guerardel, Y., Kremer, L., Barbry, P., Puzo, G., Altare, F. (2007) *Mycobacterial lipomannan* induces granuloma macrophage fusion via a TLR2-dependent, A. *J. Immunol.* **178,** 3161–3169.
63. Nigou, J., Vasselon, T., Ray, A., Constant, P., Gilleron, M., Besra, G. S., Sutcliffe, I., Tiraby, G., Puzo, G. (2008) Mannan chain length controls lipoglycans signaling via and binding to TLR2. *J. Immunol.* **180,** 6696–6702.
64. Khoo, K. H., Dell, A., Morris, H. R., Brennan, P. J., Chatterjee, D. (1995) Inositol phosphate capping of the nonreducing termini of lipoarabinomannan from rapidly growing strains of *Mycobacterium*. *J. Biol. Chem.* **270,** 12380–12389.
65. Venisse, A., Berjeaud, J. M., Chaurand, P., Gilleron, M., Puzo, G. (1993) Structural features of lipoarabinomannan from *Mycobacterium bovis* BCG. Determination of molecular mass by laser desorption mass spectrometry. *J. Biol. Chem.* **268,** 12401–12411.
66. Gilleron, M., Himoudi, N., Adam, O., Constant, P., Venisse, A., Rivière, M., Puzo, G. (1997) *Mycobacterium smegmatis* phosphoinositols-glycerooarabinomannans. Structure and localization of alkali-labile and alkali-stable phosphoinositides. *J. Biol. Chem.* **272,** 117–124.
67. Khoo, K. H., Tang, J. B., Chatterjee, D. (2001) Variation in mannose-capped terminal arabinan motifs of lipoarabinomannans from clinical isolates of *Mycobacterium tuberculosis* and *Mycobacterium avium* complex. *J. Biol. Chem.* **276,** 3863–3871.

KEY WORDS:
monocyte · paratuberculosis · lipopolysaccharide · lipoglycan · p38 mitogen-activated protein kinase · post-transcriptional gene regulation